Second Conference on Smart Monitoring,
Assessment and Rehabilitation of Civil Structures

SMAR 2013

Flexural response of RC beams strengthened by MF-FRP laminates: numerical modeling

E. Martinelli[1], A. Napoli[1], B. Nunziata[1], and R. Realfonzo[1]

[1] Department of Civil Engineering, University of Salerno, Fisciano (SA), Italy

ABSTRACT: A Finite-Element model has been developed for simulating the behaviour of RC beams strengthened in bending by Mechanically Fastened Fiber Reinforced Polymer laminates. The model has been used for simulating experimental tests collected in a wide database presented in this paper. The numerical simulations were primarily devoted to investigate the effect of the partial interaction between concrete and FRP laminate and, then, to explore other specific aspects of the mechanical behavior, such as the cracking process RC members resulting in the well-known tension stiffening effect.

1 INTRODUCTION

Several analytical and numerical studies have been carried out through years with the aim to predict the behavior of RC members strengthened in bending with Mechanically Fastened Fiber Reinforced Polymer (MF-FRP) systems: a state-of-the-art review on this topic has been recently published in Napoli et al. (2013). As highlighted therein, the first analytical models were based, for the sake of simplicity, on the hypothesis of “conservation of plane sections” between the concrete and the FRP, as generally accepted for externally bonded (EB) FRP strengthened members. Despite their ease of application, such models have often provided inaccurate predictions which were primarily attributed to ignoring the slip between the concrete and FRP strip. Therefore, novel proposals accounting for the concrete-FRP interfacial behavior were recently formulated by some authors (Lee et al. 2009, Nardone et al. 2011).

Finite element (FE) models were also developed to simulate the behavior of MF-FRP strengthened RC beams and slabs. To this aim, in a first work Napoli et al. (2010) formulated a FE procedure in which the modeling of the interface was devised by assuming a continuous connection between the FRP laminate and RC beam. Although this assumption led to results as accurate as in the case of EB-FRP systems, it introduced a certain level of approximation, especially in the case of either coarse or unequally spaced fasteners. Thus, the authors have recently developed a novel FE model which is based on the explicit assumption of discrete connection between concrete and FRP. Such model, already detailed in Martinelli et al. (2012), is used in this study to simulate experimental tests available in the literature and relative to MF-FRP strengthened RC beams and one-way slabs; these tests are part of a more general database recently published in Brown et al. (2011). The numerical simulations were mainly aimed to investigate the effect of the partial interaction between concrete and FRP strip and, then, to explore the cracking process in RC members which is often disregarded in modeling methods.

2 OUTLINE OF THE 1D-FE MODEL

Figure 1a depicts the 1D finite element formulated for simulating the flexural behaviour of RC beams externally strengthened by MF-FRP (Martinelli et al. 2012). It is obtained by assembling the following three components: a) a 1-D element that models the behavior of an Euler-Bernoulli RC beam; b) a rod element that simulates the mechanical behavior of an FRP laminate; c) two springs used as axial constrains between the FRP strip and the RC beam. The two springs simulate the behavior of the fasteners connecting the FRP laminate to some points of the beam intrados, i.e., where the fasteners are actually installed.

The aforementioned model requires the definition of the stiffness matrix of the generic finite element, whose relevant displacement and force components are reported in Figure 1b. Nonlinear relationships are introduced to model the behavior of structural materials and the response of fasteners. Figure 2a and 2b, depict the generalized stress-strain laws adopted for concrete in compression (Popovics 1973) and tension (Okamura et al. 1985) and steel rebars, respectively, whereas the FRP strip was simulated through an elastic-brittle behavior. Figure 2c, instead, shows the bearing stress-interface slip (σ-s) relationships employed to simulate the response of the connecting devices, i.e. of shot or screwed fasteners. In particular, the trilinear laws - selected in the case of screws w/ and w/o washers (models 1 and 2) - are those proposed by the authors in a previous study (Realfonzo et al. 2013); the other ones, used in the case of shot or screwed fasteners w/ washer (models 3 and 4) - are those found by Elsayed et al. (2009).

Finally, the nonlinear procedure implemented for employing the proposed finite element is based on an incremental algorithm with iterative search of the numerical solution, whereas the global model of the RC beam strengthened with MF-FRP is assembled according to well-known procedures of the finite element method (Bathe 1996). The numerical iterations within the single analysis step are continued up to achieving a given tolerance between prediction and correction; the analysis ends up when the (conventional) failure condition is achieved in either the fastening system or one of the structural materials (concrete, steel or FRP).

3 THE DATABASE

The database includes 62 four point-bending tests performed on RC beams or slabs strengthened with MF-FRP laminates, according to the test configuration shown in Figure 3. Table 1 summarizes relevant geometrical and mechanical properties of the considered specimens, whereas Table 2 provides information about the MF-FRP strengthening layouts.

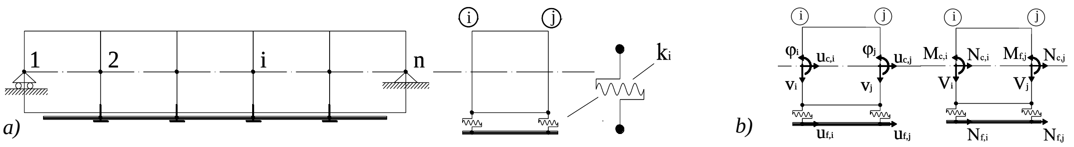

Figure 1. FEM model of a generic MF-FRP strengthened RC beam.

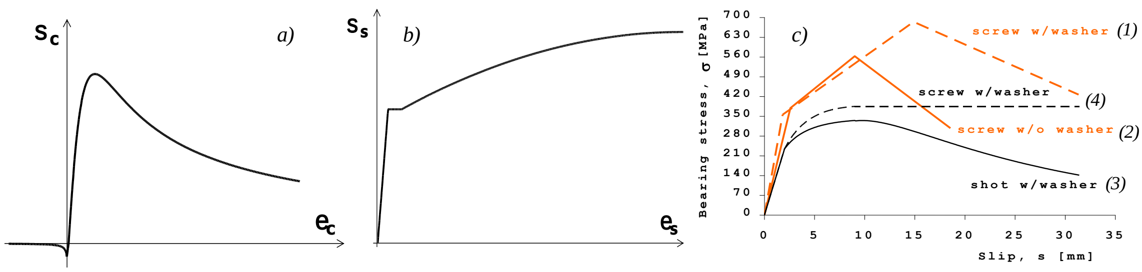

Figure 2. Nonlinear relationships adopted for concrete (a), steel rebars (b) and fasteners (c).

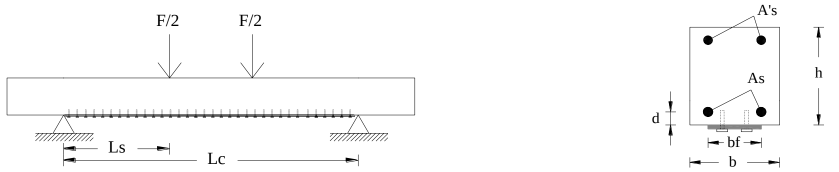

Figure 3. Test configuration.

In addition to the symbols clarified in Figure 3, the average cylinder compressive strength of concrete f_c, the length, the average elastic modulus and tensile strength of the employed FRP strip (L_f, E_f, f_f, respectively), the diameter (d_a) and the shank length (L_a) of the fasteners (shot, screw or wedge) w/ or w/o washer are mentioned in the following. The fasteners were arranged on single or multiple rows (1, 2, 4) according to aligned ("-a") or staggered ("-s") configurations or combinations thereof ("a-s"). Regarding the steel reinforcement type, Table 1 reports the average values of the yield strength (f_y) obtained in some tensile tests performed by the authors. It is noted that the specimen S-4-F (Ekenel et al. 2005) was pre-cracked prior to be MF-FRP strengthened by using wedge anchors coupled with end anchor spikes; it was subjected to a cyclic test unlike the other 61 tests, all monotonic. For the specimen M-F-P-2 (Galati et al. 2007), the FRP laminate was both bonded and mechanically fastened to the concrete substrate.

4 APPLICATION OF THE FE MODEL

The FE model has been used for performing numerical simulations of experimental tests collected in the database of Table 2. It is worth highlighting that these analyses were mainly devoted to investigate some specific aspects of the structural response which may have a varying significance in the modeling of MF-FRP strengthened beams. In particular, the influence of the following aspects was explored: *a)* uncertainty on the actual mechanical properties of steel rebars and mainly on the f_y value, which is not always provided in the literature papers, and choice of the stress-strain law to use for simulating the response of such rebars; *b)* selection of the bearing stress-slip interface law to model the effect of the partial interaction concrete and FRP laminate; and *c)* cracking process in RC members, related to a different tensile response of concrete, which is generally neglected in the modeling methods.

4.1 Influence of mechanical properties and stress-strain behavior of steel rebars

As shown in Table 2, many papers do not provide the actual mechanical properties of the used rebars, as obtained by tensile tests, but only indicate the denomination of the employed steel according to the ASTM Specifications. Thus, some mismatches between experiments and predictions may be related to uncertainties on steel rebars' properties and mainly on the yield strength value, f_y. Figures 4a,b depict the numerical simulations obtained for three tests, namely P-1, 1 and 2. For these analyses, the behavior of the steel rebars was modeled according to the stress-strain relationship of Figure 2b and by plugging two alternative values of the yield strength, i.e.: f_y = 420 MPa, which is the lowest strength attributable to the Grade 60-steel, and a slightly increased value equal to 475 MPa; then, an ultimate strength f_t = 1.2 f_y was always considered. In these tests, the concrete-FRP interface was modeled through the σ-s law proposed by Elsayed et al. (2009), which is the only available for the case of shot fasteners.

The comparisons of Figures 4a,b highlight the good accuracy of the performed modeling, thus implying that uncertainties on the steel rebars' properties are well covered by the range chosen for f_y. In fact, for the test P-1, the numerical simulation obtained by considering f_y = 420 MPa well reproduces the experimental curve in terms of initial stiffness but underestimates the flexural response at the peak condition; conversely, the numerical curve resulting from f_y = 475

MPa better approximates the post-yield behavior. By looking at the plot of Figure 4b, instead, it is noted that each numerical simulation accurately reproduces one of the two experimental curves; such curves differ each other for the length of the used fastener (L_a = 25 mm or 32 mm).

Table 1. Geometry and mechanical properties of considered test specimens.

Source	Test	L_c (mm)	L_s (mm)	b x h (mm)	A'_s (mm^2)	A_s (mm^2)	d (mm)	f_c (MPa)	Steel Type f_y (MPa)
Borowicz (2002)	U-W-2	3505	1372	305x305	143	1013	51	44.7	Grade 60
	U-W-4	2134	686						
	U-W-5	2642	940						
	U-W-6	3353	1295						
	U-W-7	3454	1346						
	U-W-8	3505	1372						
	U-W-9	3505	1372						
Ebead (2011)	M-F-10-1	2250	850	150x250	101	157	25	41	540
	M-F-10-2					157	25	38	540
	M-F-12-1					226	26	38	550
	M-F-12-2					226	26	39	550
	M-F-16-1					402	28	40	530
	M-F-16-2					402	28	39	530
	M-P-10-1					157	25	37	540
	M-P-10-2					157	25	38	540
	M-P-12-1					226	26	36	550
	M-P-12-2					226	26	39	550
	M-P-16-1					402	28	36	530
	M-P-16-2					402	28	41	530
Ekenel et al. (2005)	S-4-F	1829	304	254x165	143	214	45	27.6	414
Galati et al. (2007)	M-F-P-2	2200	600	200x250	226	226	29	31.5	462
Lamanna (2002)	D-1	1168	483	153x153	143	254	50	42	Grade 60
	D-2	1168	483					42	
	E-1	1168	483					42	
	E-2	1168	483					42	
	J-1	1168	483					42	
	L-1	1067	432					42	
	T-1	1067	432					42	
	T-2	1067	432					42	
	T-3	1067	432					42	
	F-1	1168	483					21	
	G-1	1168	483					21	
	K-1	1168	483					21	
	M-1	1067	432					21	
	N-1	1067	432					21	
	P-1	1067	432					21	
	Q-1	1067	432					21	
	R-1	1067	432					21	
	R-2	1067	432					21	
Lamanna et al. (2001)	F-42-S-102-1R	1067	432	153x153	143	254	39	42	Grade 60
	F-21-S-102-1R							21	
Lamanna et al. (2004)	S-4-Y-AL32	3353	1118	305x305	143	1013	51	35.3	Grade 60
	I-4-N-AL32								
	I-4-Y-AL32								
	I-4-Y-AL32-R								
	I-8-Y-AL32								
	H1.5-4YAL32								
	H1.5-4YAL42D								
	H1.5-4YAL47D								
	H1.5-4YAL47D-3								
	H1.5-4YAL47D-3R								
	H1.0-4YAL47D-5								
Lee et al. (2007)	1	1370	610	200x150	157	226	40	34.5	Grade 60
	2	1370	610	200x150	157	226	40	34.5	Grade 60
Martin et al. (2008)	6-L	3353	1219	305x305	143	1013	51	48	Grade 60
	6-S								
	10-L								
	12-L								
Napoli et al. (2008)	MF-1-L	3048	1219	305x152	-	380	25	26.7	Grade 60
	MF-1-S								
	MF-2-L								
	MF-2-S								

Table 2. Details on strengthening layouts.

Source	Test	b_f (mm)	t_f (mm)	L_f (mm)	E_f (GPa)	f_f (MPa)	Fastener type	d_a (mm)	L_a (mm)	Washer	# rows
	U-W-2			3404		494					2-a
	U-W-4			2134		494					2-a
	U-W-5		3.2	2642		494					2-a
Borowicz (2002)	U-W-6	102		3251	56.5	743	PAF	4.5	47	YES	2-a
	U-W-7			3048		743					2-a
	U-W-8			2997		743					2-a
	U-W-9		6.4	3404		743					2-a
	M-F-10-1			2200							2-a
	M-F-10-2			2200							2-s
	M-F-12-1			2200							2-a
	M-F-12-2			2200							2-s
	M-F-16-1			2200							2-a
Ebead (2011)	M-F-16-2	102	3.2	2200	72	1003	Screw	4.76	37	YES	2-s
	M-P-10-1			1350							2-a
	M-P-10-2			1350							2-s
	M-P-12-1			1350							2-a
	M-P-12-2			1350							2-s
	M-P-16-1			1350							2-a
	M-P-16-2			1350							2-s
Ekenel et al. (2005)	S-4-F	102	3.2	1778	62	531	Wedge	9.5	40.3	YES	1-s
Galati et al. (2007)	M-F-P-2	102	3.2	2100	62	835	Wedge	12	100	YES	1-s/2-a
	D-1			1016	13.8	232		4	22		2-a
	D-2			1117	13.8	232		4	22		2-a
	E-1			1117	13.8	232		4	22		2-a
	E-2			1117	13.8	232		4	22		2-a
	J-1			1117	13.8	232		3.7	27		1-a
	L-1			1016	13.8	232		4.5	32		1-a
	T-1		3.2	1016	13.8	232		3.7	32		1-a
	T-2			1016	13.8	232		3.7	32		1-a
Lamanna (2002)	T-3	102		1016	13.8	232	PAF	3.7	32	YES	1-a
	F-1			1117	13.8	232		3.7	27		1-a
	G-1			1117	13.8	232		3.7	27		2-a
	K-1			1117	13.8	232		3.7	32		1-a
	M-1			1016	13.8	232		3.7	32		1-a
	N-1			1016	17	351		3.7	32		1-a
	P-1		6.4	1016	15.5	204		3.7	32		1-a
	Q-1			1016	27.3	561		3.7	32		1-a
	R-1		3.2	1016	13.8	232		3.5	27		2-a
	R-2			1016	13.8	232		3.5	27		2-a
Lamanna et al. (2001)	F-42-S-102-2R	102	3.2	1016	13.8	232	PAF	3.5	27	YES	2-a
	F-21-S-102-1R							3.7	32		1-a
	S-4-Y-AL32	102			15.2	325			32		2-a
	I-4-N-AL32	102			26.3	695			32		2-a
	I-4-Y-AL32	102			26.3	695			32		2-a
	I-4-Y-AL32-R	102			26.3	695			32		2-a
	I-8-Y-AL32	204			26.3	695			32		4-a
Lamanna et al. (2000)	H1.5-4YAL32	102	3.2	3048	57.2	828	PAF	4.5	32	YES	2-a
	H1.5-4YAL42D	102			57.2	828			42		2-a
	H1.5-4YAL47D	102			57.2	828			47		2-a
	H1.5-4YAL47D-3	102			57.2	828			47		2-a
	H1.5-4YAL47D-3R	102			57.2	828			47		2-a
	H1.0-4YAL47D-5	102			56.9	916			47		2-a
Lee et al. (2007)	1	102	3.2	1370	68.3	848	PAF	3.5	25	YES	2-a
	2	102	3.2	1370	68.3	848	PAF	3.5	32	YES	2-a
	6-L										1-a
Martin et al. (2008)	6-S	102	3.2	3251	57.7	805	Screw	12.7	50.8	YES	1-s
	10-L										1-a
	12-L										1-a
	MF-1-L			2718							1-s
Napoli et al. (2008)	MF-1-S	102	3.2	2108	62	852	Screw	9.5	44.5	NO	1-s
	MF-2-L			2718							1-s
	MF-2-S			2413							1-s

A further aspect of interest in the modeling of the steel rebars' behavior deals with the approximation level achieved when an elastic-perfectly plastic stress-strain law is used in place of the more accurate one shown in Figure 2b. To this aim, Figure 4c confirms a rather slight dependence of the numerical curves on the model type used for steel rebars; therefore, the elastic-perfectly plastic law can be successfully chosen for the simulations of all tests.

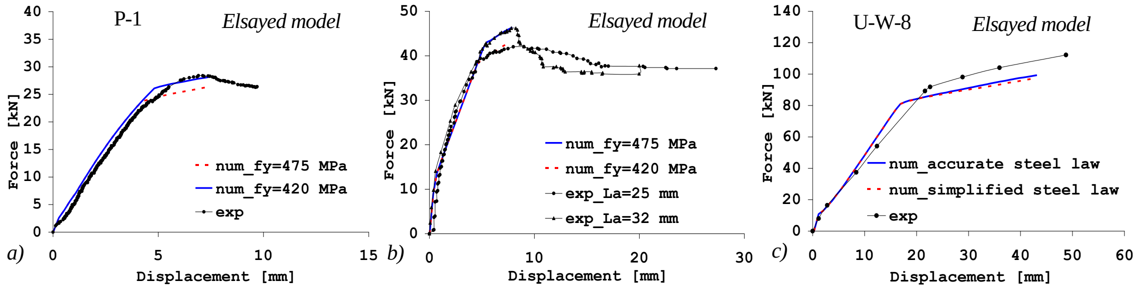

Figure 4. Influence of the mechanical properties (a,b) and stress-strain law (c) of steel rebars.

4.2 *Influence of the bearing stress-slip interface law*

As mentioned earlier, Elsayed et al. (2009) and Realfonzo et al. (2013) recently proposed nonlinear bearing stress-slip models to describe the effect of the partial interaction between the concrete and the FRP laminate. These models, depicted in Figure 2c, were experimentally calibrated through direct shear (DS) tests performed on MF-FRP/concrete joints with a single connector. In particular, among the proposals by Elsayed et al., one model was found from joints having a shot fastener with a 47 mm shank length, a 3.7 mm shank diameter and a 13 mm washer; the other one, instead, was defined for a screwed fastener with a 37 mm shank length, a 4.8 mm shank diameter and a 16 mm washer. The trilinear models proposed by Realfonzo et al. were found from a screwed fastener with (w/) or without (w/o) washer; the screw adopted in the DS tests had a 45 mm shank length, a 6 mm shank diameter and a 32 mm washer (when used).

Comparisons between experimental and numerical force-deflection curves are shown in Figure 5 which allow to better investigate the sensitivity of the structural response with the use of different bearing stress-slip relationships. In the plots of Figures 5a-c the behavior of the screws w/ washer was modeled by using the respective σ-s laws provided by Elsayed et al. ("Elsayed model") and Realfonzo et al. ("Trilinear model"). As observed, both simulations well reproduce the initial stiffness of the experimental curves since the two bearing stress-slip models overlap each other for low values of interfacial slips (Fig. 2c). Then, at increasing the relative displacement between the concrete and FRP strip, a greater force per fastener is calculated with the trilinear σ-s law which in turn leads to overestimate the flexural strength of the beams.

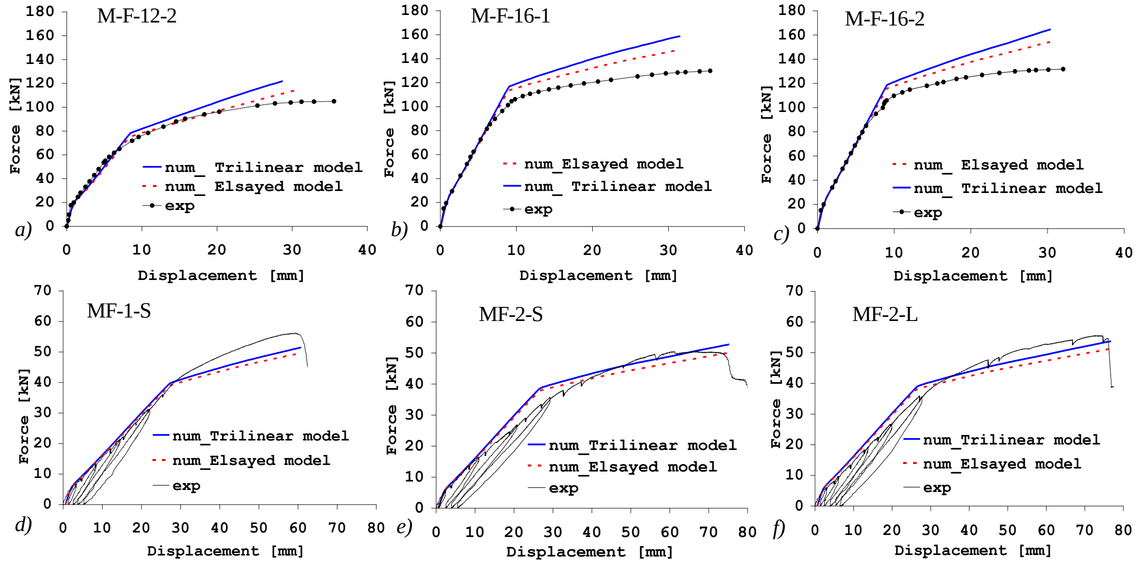

Figure 5. Influence of the bearing stress-slip law.

Thus, although differences between the two simulations are rather negligible, the numerical predictions obtained by assuming the "Elsayed model" better predict the three experimental curves; this evidence may be partially justified by the fastener type used in the tests by Ebead (2011) which is the same employed by Elsayed et al. in the DS tests. Figures 5d-f, instead, the behavior of screws w/o washer was modeled by using the trilinear law by Realfonzo et al. and, as a comparison, the one by Elsayed et al., though suitable for fastener w/ washer. In the case of the test MF-1-S, the Figure shows a very good agreement between experimental results and numerical predictions which are rather accurate in simulating the cracking onset in concrete and yielding in steel rebars. In the cases of tests MF-2-L and MF-2-S, the numerical responses before steel yielding are characterized by a slightly greater stiffness with respect to the experimental ones. In all cases, since small values of interfacial slips are activated for these members, the numerical simulations do not significantly change with the use of the two σ-s relationships, thus implying that both of them are suitable to model MF-FRP strengthened slabs.

4.3 Influence of the tension-stiffening effect

The simulation of the cracking processes of RC members is a challenging issue, especially in the case of 1D numerical models. Such processes are characterised by the onset of cracking in concrete subjected to tensile stresses: since the actual tensile strength of concrete is generally affected by significant levels of randomness, the prediction of the cracking onset is often a critical issue. Also, the well-known tension-stiffening effect significantly influences the flexural response of RC members in the post-cracking stage. Since the present proposal is based on a continuous (smeared) crack FE model, the tension stiffening effect can be simulated by a conventional softening branch in the tensile stress-strain law of concrete (Okamura et al. 1985):

$$\sigma_c = f_{ct} \cdot \left(\frac{f_{ct}/E_{ct}}{|\varepsilon|} \right)^C \quad \text{with } \varepsilon < f_{ct}/E_{ct} \qquad (1)$$

where f_{ct} is the nominal tensile strength, E_{ct} the Young modulus of concrete in tension and C a conventional exponent which needs to be duly calibrated on experimental results.
In this study, the tension stiffening effect is investigated by considering three fairly different values of such C exponent, spanning over a range from 0.5 to 50 and covering tensile behaviors of concrete from rather resilient (C=0.5) to very brittle (C=50). Figure 6 shows the resulting numerical simulations for some tests; it is noted that the effect of a different tensile response of concrete is particularly relevant in terms of flexural stiffness in the post-cracking regime. However, a lower tension-stiffness effect (simulated by assuming C=50) has an influence on the bending moment of the beam at yielding. Particularly, it results in the most accurate simulations in terms of initial stiffness when shot fasteners are used (see Figs 6a,b). In fact, the installation of such connector type generally induces significant pre-cracking in the concrete which is well reproduced by a lower contribution of the tension-stiffening effect.

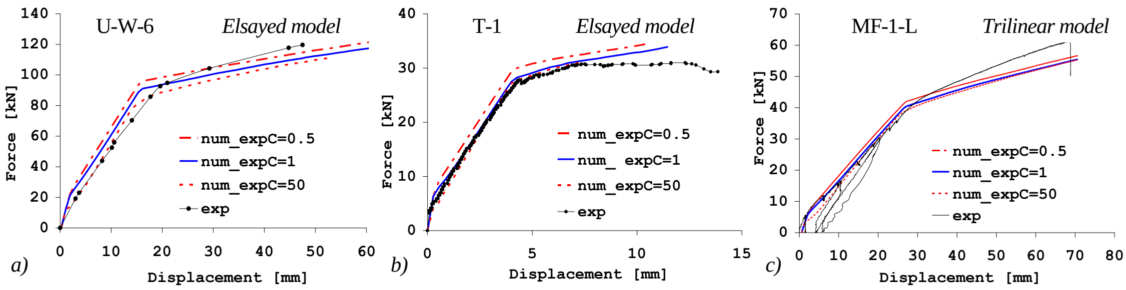

Figure 6. Influence of the tension-stiffening effect.

5 CONCLUSIONS

A finite element model was developed and used by the authors to simulate the flexural behaviour of RC beams externally strengthened by mechanically fastened FRP laminates. The numerical analyses allowed to investigate the influence of some specific aspects on the structural response of MF-FRP strengthened members, such as: stress-strain laws of steel rebars, bearing stress-slip law assumed for the FRP-concrete interface, and the cracking process, with emphasis to the tension stiffening effect developing in RC members. The considerations drawn from this study will be employed in future developments of this research which is aimed to calibrate sound design rules and criteria for strengthening existing RC beams through mechanically fastened FRP systems.

6 REFERENCES

Bank, LC, and Arora, D. 2006. Analysis of RC beams strengthened with mechanically fastened FRP (MF-FRP) strips. *Composite Structures*, 79: 180-191.

Bathe, KJ. 1996. Finite Element Procedures. Prentice Hall Inc., New Jersey, USA.

Borowicz, DT. 2002. Rapid strengthening of concrete beams with powder-actuated fastening systems and fiber reinforced polymer (FRP) composite materials. *MSc Thesis*. University of Wisconsin-Madison.

Brown, VL, Bank, LC, Arora, D, Borowicz, DT, Godat, A, Lamanna, AJ., Lee, J, Matta, F, Napoli, A, and Tan, KH. 2011. Experimental studies of mechanically-fastened FRP systems: state-of-the-art. *ACI Special Publication SP-275-48– Proc. of the FRPRCS-10*, Tampa Bay, USA, 841-86.

Ebead, U. 2011. Hybrid externally bonded/mechanically fastened fiber-reinforced polymer for RC beam strengthening. *ACI Structural Journal*, 108: 669-678.

Ekenel, M, Rizzo, A, Myers, JJ, and Nanni, A. 2006. Flexural fatigue behavior of reiforced concrete beams strengthened with FRP fabric and precured laminate systems. *J. of Comp. for Construction*, 10(5): 433-442.

Elsayed, WE, Ebead, UA, and Neale, KW. 2009. Studies of mechanically Fastened fiber-reinforced polymer strengthening systems. *ACI Structural Journal*, 106: 49-59.

Galati, D, Rizzo, A, and Micelli, F. 2007. Comparison of reinforced concrete beams strengthened with FRP pre-cured laminate systems and tested under flexural loading. *In Proc. of FRPRCS-8*, Patras.

Lamanna, AJ, Bank, LC, and Scott, DW. 2001. Flexural strengthening of reinforced concrete beams using fasteners and fiber-reinforced polymer strips. *ACI Structural Journal*, 988: 368-376.

Lamanna, AJ. 2002. Flexural strengthening of reinforced concrete beams with mechanically fastened fiber reinforced polymer strips. *PhD Thesis*. University of Wisconsin-Madison.

Lamanna, AJ, Bank, LC, and Scott, DW, A. 2004. Flexural strengthening of reinforced concrete beams by mechanically attaching fiber-reinforced polymer strips. *J. of Composite for Construction*, 8(3): 203-210.

Lee, JH, Lopez, MM, and Bakis, CE. 2009. Slip effects in reinforced concrete beams with mechanically fastened FRP strip. *Cement & Concrete Composites*, 31: 496–504.

Martin, JA, and Lamanna, AJ. 2008. Performance of mechanically fastened FRP strengthened concrete beams in flexure. *Journal of Composite for Construction*, ASCE, 12(3): 257-265.

Martinelli, E, Napoli, A, Nunziata, B, and Realfonzo, R. 2012. A Novel FE model for RC beams strengthened in bending by Mechanically Fastened FRP laminates. *In Proc. of Cice 2012*, Rome, June 14-16.

Napoli, A, Matta, F, Martinelli, E, Nanni, A, and Realfonzo, R. 2010. Modelling and verification of response of RC slabs strengthened in flexure with mechanically fastened FRP laminates. *Magazine of Concrete research*, 62(8): 593-605.

Napoli, A, Martinelli, E, Realfonzo, R, Matta, F, Bank, LC, and Brown VL. 2013. Analytical and Numerical Studies of Mechanically-Fastened FRP Systems: State-of-the-Art. Submitted to *the FRPRCS-11*, Guimarães, Portugal, June 26-28.

Nardone, F, Lignola, GP, Prota, A, Manfredi, G, and Nanni, A. 2011. Modeling of flexural behavior of RC beams strengthened with mechanically fastened FRP strips. *Composite Structures*, 93: 1973-1985.

Okamura, H, Maekawa, K, and Sivasubramaniyam, S. 1985. Verification of Modeling for Reinforced Concrete Finite Element. *Finite Element Analysis of Reinforced Concrete Structures*, ASCE:528-543.

Popovics, S. 1973. A numerical approach to the complete stress strain curve for concrete. *Cement and concrete research*, 3(5): 583-59.

Realfonzo, R, Martinelli, E, Napoli, A, and Nunziata B. 2013. Experimental investigation of the mechanical connection between FRP laminates and concrete. *Composites Part B: Engineering*, 45(1): 341-355.